J Mol Model (2006) 12: 281–289
DOI 10.1007/s00894-005-0028-4

ORIGINAL PAPER

Nadine Homeyer · Anselm H. C. Horn
Harald Lanig · Heinrich Sticht

AMBER force-field parameters for phosphorylated amino acids in different protonation states: phosphoserine, phosphothreonine, phosphotyrosine, and phosphohistidine

Received: 25 February 2005 / Accepted: 21 June 2005 / Published online: 21 October 2005

Abstract We report a consistent set of AMBER force-field parameters for the most common phosphorylated amino acids, phosphoserine, phosphothreonine, phosphotyrosine, and phosphohistidine in different protonation states. The calculation of atomic charges followed the original restrained electrostatic potential fitting procedure used to determine the charges for the parm94/99 parameter set, taking α-helical and β-strand conformations of the corresponding ACE-/NME-capped model peptide backbone into account. Missing force-field parameters were taken directly from the general AMBER force field (gaff) and the parm99 data set with minor modifications, or were newly generated based on ab initio calculations for model systems. Final parameters were validated by geometry optimizations and molecular-dynamics simulations. Template libraries for the phosphorylated amino acids in Leap format and corresponding frcmod parameter files are made available.

Keywords AMBER · Parameters · Phosphorylated amino acids · Force field · Restrained electrostatic potential

Electronic Supplementary Material Supplementary material is available for this article at http://dx.doi.org/10.1007/s00894-005-0028-4

N. Homeyer · A. H. C. Horn · H. Sticht (✉)
Abteilung für Bioinformatik, Institut für Biochemie,
Friedrich-Alexander-Universität Erlangen-Nürnberg,
Fahrstraße 17, 91054 Erlangen, Germany
E-mail: h.sticht@biochem.uni-erlangen.de
Tel.: +49-9131-8524614
Fax: +49-9131-8522485

H. Lanig
Computer-Chemie-Centrum, Nägelsbachstraße 25,
91052 Erlangen, Germany

Introduction

Phosphorylation of polypeptides is an important process governing essential steps in cellular regulatory networks. Proteins that are functionally controlled by phosphorylation and dephosphorylation are ubiquitous in prokaryotic and eukaryotic cells. It is assumed that about 30% of the proteins encoded by the human genome are phosphorylated at some point in time [1]. The post-translational, reversible phosphorylation of proteins can induce changes in their enzymatic activity, localization, and binding properties, thereby controlling, for example, catabolism and metabolism, signal transduction, growth, and gene expression [2]. Signal-transduction cascades, such as the phosphotransferase system in bacteria [3] or the mitogen activated protein-kinase cascade, play key roles in the cellular information processing network. Therefore, functioning of the phosphorylation processes in these cascades is a research subject of increasing interest.

Although abundant, protein phosphorylation is a very specific process. The phosphate can only be transferred to particular residues of a polypeptide. Phosphorylation predominantly takes place at the amino acids serine, threonine, and tyrosine. It occurs on the side-chain hydroxyl group oxygens, resulting in the formation of a phosphoester linkage between amino-acid residue and phosphate group [4]. Although not as common as serine, threonine, and tyrosine, phosphorylation on histidine residues occurs in a number of proteins. Either one of the two nitrogens in the imidazole ring can be phosphorylated, forming a phosphoramidate bond between the phosphor and a nitrogen atom. Whether Nϵ2 or Nδ1 is the target of a phosphorylation is determined by structural features of the particular molecule [5].

Since the structural properties of phosphorylated proteins are important for molecular recognition and regulatory processes, much effort is spent on the investigation of the structural features and the dynamic behavior of these molecules. Computational models

using empirical potential energy functions based on molecular mechanics (MM) principles, which have proven to be capable of giving insight into the structure and dynamics of biochemical molecules, are promising tools for studying the characteristics of phospho-proteins. These MM-based methods depend on accurate force fields properly reproducing the features and behavior of the modeled molecules. One force field widely and successfully used for the simulation of biological macromolecules such as RNA, DNA, and proteins, is AMBER [6, 7]. While the included parameters for monophosphates allow simulations of nucleosides and nucleotide oligomers [8], and parameters for the deprotonated forms of phosphotyrosine [9] and phosphothreonine [10] generated in diverse ways and for older AMBER parameter sets have been reported but not included in the AMBER distribution, a consistent set of publicly available parameters specially designed for phospho-amino acids is still lacking. Therefore, we decided to develop AMBER force-field parameters for the four most common phospho-amino-acid residues.

Computational methods

As the pK_a values of the equilibrium between the unprotonated and singly protonated phosphate group forms of the phospho-amino acids are close to pH 7 [5, 11], it can be assumed that a considerable amount of both forms exists under neutral conditions. Therefore, parameters for the anionic and dianionic phosphate group forms are required. Given the fact that histidine can be phosphorylated at two different sites, the total number of phosphorylated residues to be parameterized sums up to ten (cf. Table 1).

Calculation of restrained electrostatic potential atomic charges

Following the original procedure used to determine the atomic charges for the AMBER parm94/parm99 parameter sets [6, 7], small peptide model systems consisting of the phosphorylated amino acid residues blocked by acetyl- and *N*-methyl groups were created. The resulting ACE-XXX-NME model peptides are shown in Fig. 1.

Table 1 Listing of the analyzed phosphorylated amino acids and their charge states

	Charge of the phosphate group	Total charge	Alias[a]
Phosphoserine	−1	−1	S1P
	−2	−2	S2P
Phosphothreonine	−1	−1	T1P
	−2	−2	T2P
Phosphotyrosine	−1	−1	Y1P
	−2	−2	Y2P
Phosphohistidine (phosphorylated at ND1)	−1	0	H1D
	−2	−1	H2D
Phosphohistidine (phosphorylated at NE2)	−1	0	H1E
	−2	−1	H2E

[a]Abbreviations for the phospho-amino acids are identical with the residue names in the library and parameter files

As in the original AMBER charge-fitting procedure, two different structures of each model peptide were generated, representing the α-helical and extended (β-strand) conformations of the phospho-amino acids. Since no preferred side-chain torsion angles for the phosphorylated residues were available from the literature, and the number of phosphorylated polypeptide structures in the Protein Data Bank is too small to serve as a reliable basis set for derivating accurate χ angle distributions, it was not possible to assign specific χ values to the α-/β-conformers. Instead, initial side chains were built according to the most extended conformer. The ϕ and ψ dihedrals of the α- and β-structures were chosen according to the values used for the charge calculation of the common amino acids [12]. In order to avoid the formation of hydrogen bonds between the phosphate group and backbone atoms, the former was arranged in an extended conformation pointing away from the backbone of the model peptides. Initially all phospho-amino-acid residues were neutralized by protonating the phosphate group oxygens, thus creating ten neutral primary model system structures.

All model systems were optimized in two consecutive steps at the HF/MIDI! [13] and then the HF/6-31G(d) [14, 15] level of theory using Gaussian03 [16] with the ϕ and ψ dihedrals kept fixed. The HF/6-31G(d) method was chosen to obtain atomic charges consistent with the parm94/parm99 parameter sets [12, 17]. It has also proven to yield results particularly suitable for empirical solvent-model calculations [7]. All subsequent optimizations and single-point calculations were also performed at the HF/6-31G(d) level.

The resulting structures of the *O*-phosphorylated amino acids were reoptimized in their singly protonated form with fixed ϕ and ψ torsions. Subsequently, the remaining hydroxyl groups of the optimized, singly protonated *O*-phosphomonoester and phosphoramidate structures were fully deprotonated. Since the unprotonated phosphohistidine structures are only stable in solution and the dianionic phosphate group forms of the phospho-amino acids generally tend to adopt conformations with hydrogen bonds between phosphate group and backbone (a case that should be avoided according to the restrained electrostatic potential (RESP) charge generation recommendation [12]) in gas-phase optimizations, these systems were just partially optimized, keeping all but the phosphate group bonds, angles and torsions fixed.

The charge-derivation process was started by calculating the electrostatic potential for the optimized singly protonated and unprotonated phospho-amino-acid model system structures for all α- and β-conformers with HF/6-31G(d). Thereafter, a RESP fit was carried out [18], which was performed in three stages on the two conformations (α and β) using the RESP tool of the AMBER program suite [19]. The fit was performed

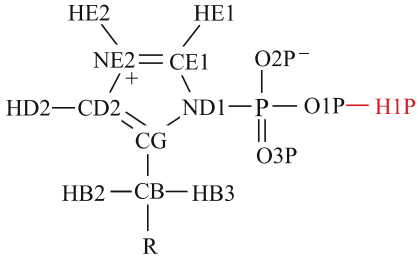

H1D / H2D

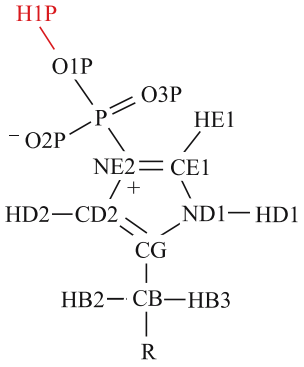

H1E / H2E

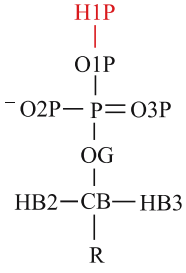

S1P / S2P

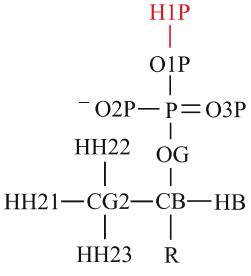

T1P / T2P

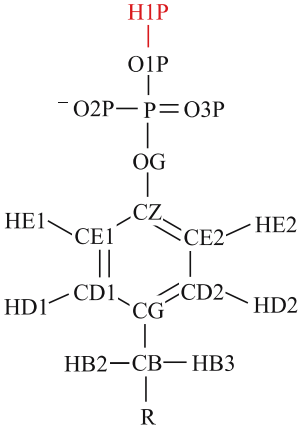

Y1P / Y2P

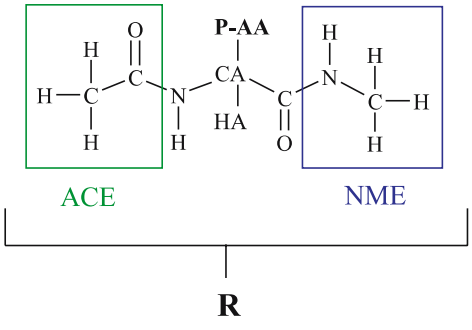

Fig. 1 Schematic illustration of the systems investigated. Acid hydrogens and corresponding abbreviations of the singly protonated phospho-amino acid residues are shown in *red*. The backbone part of the model compounds is represented by **R** (cf. lower right corner; acetyl- and *N*-methyl blocking groups are colored in *green and blue*, respectively). The atom names used correspond to the AMBER parm99 parameter set

according to the standard procedure [12] and will therefore be described here only briefly. In the first stage of the charge-fitting procedure an overall charge of 0, −1, or −2 was assigned to the phospho-amino-acid residues according to the total residue charges listed in Table 1. The charges of the ACE- and NME-blocking group atoms were constrained to their values in the parm99 parameter set, and peptide bond atom charges were frozen to the parm99 charges for neutral or anionic amino acid residues, respectively [7]. Furthermore, charges of all corresponding atoms in the α- and β-conformers were constrained to be equivalent. In the second stage, the structurally equivalent phosphate group oxygens were forced to have identical charges. The atomic charges of all atoms but unprotonated phosphate oxygens as well as alkyl/aryl carbons and hydrogens were constrained to the values from stage one. In the third stage, charges on all atoms were kept fixed except those belonging to the previously described uncharged substructures. While the charges on the carbons in unpolar groups were reoptimized in the presence of a strong hyperbolic restraint, charges on structurally equivalent carbon and hydrogen atoms were forced to be equal [7].

Determination of missing parameters

It was our intention to introduce as few new parameters as possible. However, a comparison of bonds, angles, and torsions of the ab initio optimized structures with the corresponding parm99 parameters revealed that some parameters needed to be newly defined. If feasible, these parameters were taken directly from the general AMBER force field (gaff) [20]. Table 2 shows an overview of all additional parameters and their sources.

Parameters labeled as being taken from the parm99 parameter set were modified slightly by adjusting their force constants to values suitable for phospho-amino acids. Since in test MD simulations the P-OS and P-OH bonds adopted too small values, their force constants were increased to the corresponding value of the P-O2 bond. For similar reasons the force constants of the OH-P-O2 and the HO-OH-P angles were adapted to the respective value of the O2-P-O2 angle. Force constants of the improper torsions CR-CC-NA-P and CR-CW-NA-P were set to values of the same magnitude as the force constants of analogous, improper torsions adjacent in the imidazole ring system of histidine.

Furthermore, some adaptions of the gaff parameters were necessary: the equilibrium value for the NA-P-O2 angle was changed to the respective NA-P-OH angle value, because the ab initio optimized structures possessed NA-P-O2 angles that were considerably smaller than the equilibrium value defined in gaff. Lacking parameters for the C-OS-P angle, the respective values of the ab initio optimized structures were examined. Since the determined values were close to the equilibrium value of the gaff c3-os-p5 angle, the parameters of the c3-os-p5 component were not only assigned to the analogous CT-OS-P angle but also to the C-OS-P angle. Parameters for the CA-C-OS angle were taken from the gaff ca-c-oh angle, which possesses a geometry similar to that of the CA-C-OS angle found in the ab initio optimized structures.

An entirely new parameterization was necessary for the phosphate group torsions of the phosphohistidine residues and the NA-P bond. This was performed using the phosphoimidazole substructure of the Nδ1 phosphorylated histidine compound shown in Fig. 1, in analogy to the generation of phosphohistidine parameters for GROMOS [21].

For determinating the torsion potentials, a singly protonated as well as an unprotonated phosphate group form of phosphoimidazole were geometry optimized in the same way as the peptide model systems described above. Subsequently, rotational profiles for the O2-P-NA-CC and OH-P-NA-CC dihedrals were generated. Seventy-two rotamers differing by 5° were reoptimized using Gaussian03 with the appropriate dihedral angle kept fixed. Thereafter, a MM energy calculation was performed for the corresponding rotamers. Force constants were then varied to match the rotational profiles of the ab initio calculations.

The NA-P bond-length parameter was set according to the mean distance between NA and P in the ab initio optimized singly protonated phosphohistidine structures. A force constant for the bond was calculated in accordance to the procedure recommended in the AMBER manual [22]. A bond-deformation path of the NA-P bond of singly protonated phosphoimidazole comprising eight points was calculated using Gaussian and AMBER. The bond-force constant was then determined by a least-square parabolic fit procedure [22].

Validation of the parameters by MM calculations

In order to prove the ability of the new parameters to reproduce the optimal geometries of the phospho-amino-acid residues determined quantum mechanically, minimizations of all model systems were carried out using the SANDER module of the AMBER 7.0 suite of programs [19]. The ab initio optimized model peptides were minimized in vacuo as well as in explicit water employing the parm99 parameter set augmented by the new phospho-amino-acid parameters. For the calculations in water, the charged systems were neutralized by adding Na^+ counterions. The neutral systems were then placed in a TIP3P [23] water box with at least a 10 Å distance between the solute and the border of the box.

Convergence criterion for all minimizations was a root-mean-square energy gradient value of less than 0.1 kcal mol^{-1} $Å^{-1}$. Gas-phase calculations were conducted using 250 steps of steepest descent minimization followed by at least 600 steps of the conjugate gradient method. Minimizations of the solvated model peptides were started by relaxing the solvent molecules while the solute atoms were kept fixed. After 2,000 steps of solvent relaxation, a 250-step steepest descent minimization of the whole system was performed. Then the minimization method was changed to conjugate gradient, which was carried out until the convergence criterion was reached.

In order to analyze the performance of the new parameters, MD simulations of the model peptides in aqueous solution were carried out. Prior to the MD runs, the model systems generated for the aqueous minimizations were subjected to 2,000 steps of solvent relaxation and 5,000 steps of free minimization using the steepest descent as well as the conjugate gradient methods. Subsequently, an equilibration run of 70 ps was carried out raising the temperature to 300 K and the density to a value of approximately 1 g cm^{-3}. MD simulations were performed at 300 K and 1 bar under NPT conditions using periodic boundary conditions and a time step of 1 fs. A dielectric constant of 1 and a 10 Å cutoff distance were assigned, and SHAKE constraints were applied. The data collection took place in time intervals of 1 ps. Every simulation was carried out for a total of 1 ns.

Table 2 New parameters assigned to the phosphorylated amino acids

Bonds	Atom types	r_{eq}^{a}	K_r^{b}	Phospho-amino acid
P-[ND1/NE2]	P-NA	1.840 (C)	250.0 (C)	H1D, H2D, HIE, H2E
P-OG	P-OS	1.610 (P)	525.0 (P)	S1P, S2P, T1P, T2P, Y1P, Y2P
P-O1P	P-OH	1.610 (P)	525.0 (P)	H1D, H1E, S1P, T1P, Y1P

Angles	Atom types	Θ_{eq}^{a}	K_Θ^{b}	Phospho-amino acid
CG-ND1-P	CC-NA-P	125.10 (G)	76.7 (G)	H1D, H2D
CE1-[ND1/NE2]-P	CR-NA-P	125.10 (G)	76.7 (G)	H1D, H2D, H1E, H2E
CD2-NE2-P	CW-NA-P	125.10 (G)	76.7 (G)	H1E, H2E
[ND1/NE2]-P-OXP[c]	NA-P-O2	102.38 (G)	42.9 (G)	H1D, H2D, H1E, H2E
[ND1/NE2]-P-O1P	NA-P-OH	102.38 (G)	42.9 (G)	H1D, H1E
O1P-P-OXP[c]	OH-P-O2	108.23 (P)	140.0 (P)	H1D, H1E, S1P, T1P, Y1P
H1P-O1P-P	HO-OH-P	108.50 (P)	140.0 (P)	H1D, H1E, S1P, T1P, Y1P
CB-OG-P	CT-OS-P	120.50 (G)	100.0 (G)	S1P, S2P, T1P, T2P
CZ-OG-P	C-OS-P	120.50 (G)	100.0 (G)	Y1P, Y2P
[CE1/CE2]-CZ-OG	CA-C-OS	120.00 (G)	70.0 (G)	Y1P, Y2P

Torsions	Atom types	$V_n/2^{d}$	γ^{e}	n^{f}	Phospho-amino acid
CG-ND1-P-OXP[c]	CC-NA-P-O2	0.24 (C)	0.0	3	H1D, H2D
CD2-NE2-P-OXP[c]	CW-NA-P-O2	0.24 (C)	0.0	3	H1E, H2E
CG-ND1-P-O1P	CC-NA-P-OH	1.45 (C)	0.0	2	H1D
CD2-NE2-P-O1P	CW-NA-P-OH	1.45 (C)	0.0	2	H1E

Improper torsions	Atom types	$V_n/2^{d}$	γ^{e}	n^{f}	Phospho-amino acid
CE1-CG-ND1-P	CR-CC-NA-P	1.10 (P)	180.0	2	H1D, H2D
CE1-CD2-NE2-P	CR-CW-NA-P	1.10 (P)	180.0	2	H1E, H2E

Parameters derived from gaff or parm99, or parameterized anew are designated (G), (P), or (C), respectively
[a] Equilibrium distance or angle in (Å) or (°)
[b] Force constant for bond or angle in (kcal mol^{-1} Å^{-2}) or (kcal mol^{-1} rad^{-2})
[c] Phosphate group oxygens not bound to an hydrogen atom
[d] Torsion potential in (kcal mol^{-1}). The number of bond paths that $V_n/2$ is divided into is 1
[e] Phase offset in (°)
[f] Periodicity of the torsion

Results and discussions

Parameterization

Following the strategy to ensure compatibility with the present AMBER settings by defining as few new parameters as possible, the parameterization was limited to completely missing or inappropriate equilibrium values and force constants. However, to provide force-field parameters suitable for accurate simulations of polypeptides containing phosphoserine, phosphohistidine, phosphotyrosine, or phosphothreonine residues, it was nevertheless necessary to modify or add 19 sets of parameters (Table 2).

The majority of force constants and equilibrium values were adapted from available AMBER parameters in order to stay consistent with the parm99 parameter set. Furthermore, because gaff was designed as an extension of the existing AMBER force fields for organic molecules [20], it is reasonable to take and adapt the already available parameters.

Determination of parameters not present in gaff and not resembling any structural object defined in the parm99 parameter set was performed using well-established procedures. Calculation of the P-NA force constant by the method recommended in the AMBER manual yielded a value of 250 kcal mol^{-1} Å^{-2}. Ab initio calculations of the dianionic phosphate group forms of *N*-phosphorylated amino acids as well as analysis of phosphohistidine stability [4] showed that the P-NA bond is considerably weaker than the P-O bond in *O*-phosphorylated amino acids. Since the force constant assigned to the P-O2 bond in the parm99 parameter set is 525 kcal mol^{-1} Å^{-2}, the value determined for the P-NA bond is reasonable.

AMBER parameters for the rotation around the P-N bond were determined by calculating the ab initio and MM energies of the unprotonated and protonated phosphoimidazole for a set of fixed O2-P-NA-CC and OH-P-NA-CC torsion values. The O2-P-NA-CC ab initio energy profile showed three symmetrically arranged minima and maxima with almost identical

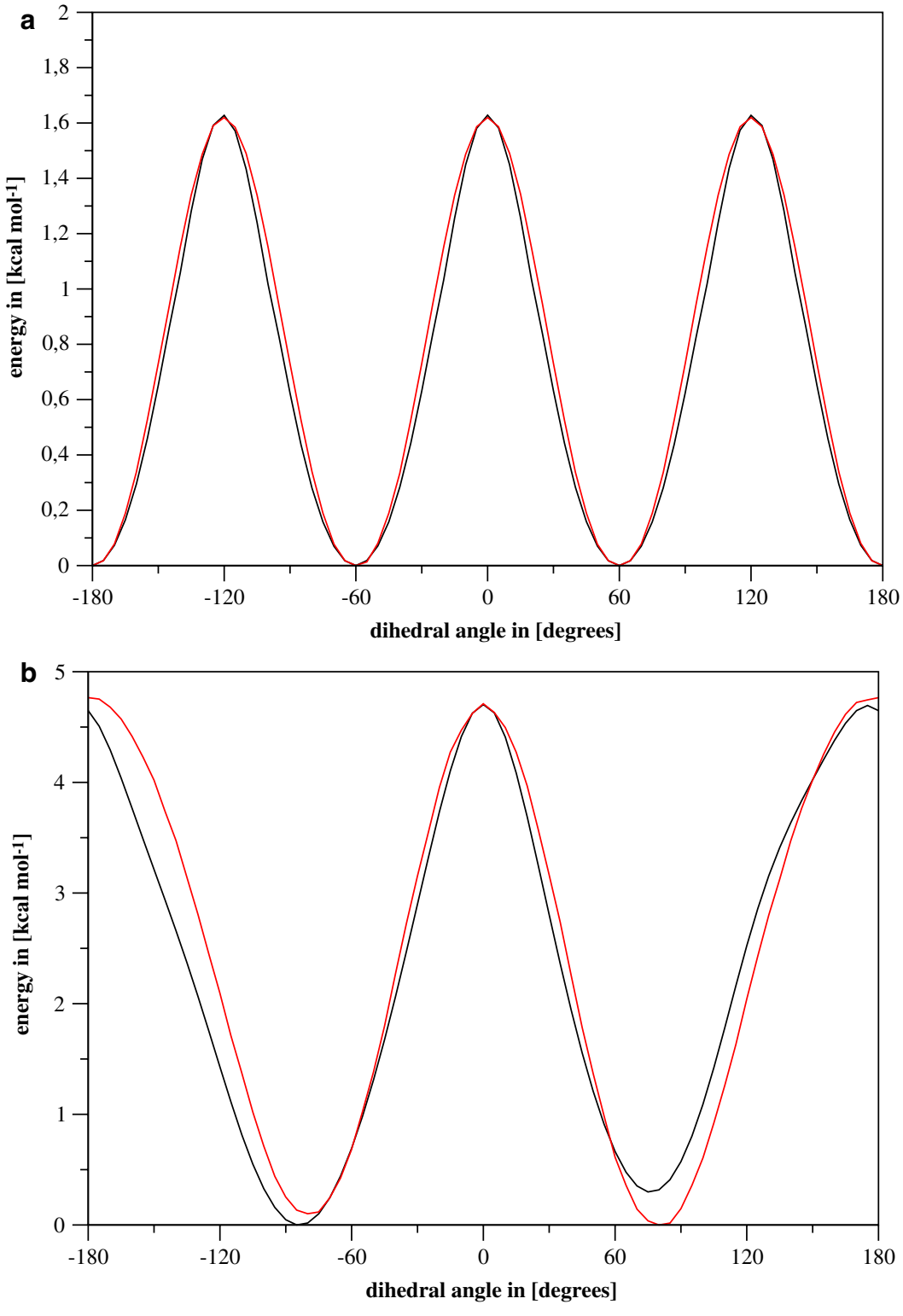

Fig. 2 Ab initio (*black*) and AMBER (*red*) rotational profile of phosphoimidazole; (**a**) deprotonated form, dihedral angle O2-P-NA-CC; (**b**) protonated form, dihedral angle OH-P-NA-CC

absolute values (Fig. 2), intervals between two extrema were approximately 60° wide, which is the expected behavior of a freely rotating PO_3^{2-} group.

In finding parameters that reproduce the ab initio energy profile properly, the fitting procedure for the AMBER O2-P-NA-CC dihedral yielded an energy curve

Table 3 Comparison of ab initio (gas phase) and AMBER (gas phase and water) optimized structures: sample geometrical parameters comprising all new parameterized bond lengths and angles of phosphoserine (S1P and S2P) and ND1-phosphorylated phosphohistidine (H1D and H2D)

Bond, angles[a,b]	Ab initio (α-/β-conformers)	AMBER (gas phase)	AMBER (water)	AMBER parameters
S1P				
P-OS	1.657/1.656	1.60	1.60	1.61
P-OH	1.633/1.638	1.58	1.58	1.61
OS-P-O2	107.2; 105.1/107.9; 104.6	109.8; 109.2	110.9; 109.8	108.23
OH-P-O2	107.8; 108.2/108.2; 107.1	106.2; 106.5	105.6; 105.5	108.23
OH-P-OS	99.7/99.6	103.7	101.5	102.60
P-OH-HO	107.6/107.2	103.7	103.6	108.50
CT-OS-P	119.4/121.0	120.8	121.5	120.50
S2P				
P-OS	1.657/1.656	1.61	1.59	1.61
OS-P-O2	100.9; 103.0; 102.0/103.6; 99.7; 102.3	103.2; 102.6; 102.5	105.2; 106.5; 105.4	108.23
CT-OS-P	117.3/120.3	119.8	118.5	120.50
HID				
P-NA	1.839/1.828	1.83	1.84	1.84
P-OH	1.604/1.602	1.59	1.59	1.61
CC-NA-P	130.0/130.6	127.8	128.1	125.10
CR-NA-P	121.4/121.0	124.6	125.0	125.10
NA-P-O2	100.7; 103.6/104.6; 101.2	109.3; 104.4	109.2; 107.0	102.38
NA-P-OH	98.1/98.3	106.4	107.9	102.38
OH-P-O2	110.3; 110.0/109.0; 110.7	107.5; 107.0	105.5; 107.4	108.23
HO-OH-P	110.8/111.2	104.8	104.9	108.50
H2D				
P-NA	1.839/1.828	1.84	1.85	1.84
CC-NA-P	126.9/127.4	129.2	129.0	125.10
CR-NA-P	124.5/124.3	123.6	123.9	125.10
NA-P-O2	99.1; 96.8; 98.5/99.4; 100.5; 97.2	97.8; 96.9; 99.7	101.3; 101.1; 109.8	102.38

[a] For the corresponding atom names and their occurrence see Table 2 and Fig. 1
[b] Bond length values in (Å), bond angles in (°)

almost congruent with the quantum mechanical one. The small root-mean-square deviation of 0.066 kcal mol^{-1} between the two curves confirms the quality of the determined parameters.

Using these O2-P-NA-CC dihedral parameters and a protonated phosphoimidazole model system the fitting procedure was repeated for the OH-P-NA-CC dihedral. The ab initio energy profile of that torsion possesses two unequally distributed minima and maxima, as reported previously [21]. Thus, a periodicity of 2 was chosen for the OH-P-NA-CC torsion to match the ab initio values. In the fitting procedure, care was taken that the MM barrier of rotation was of similar magnitude as the reference value, and so the final root-mean-square deviation of 0.376 kcal mol^{-1} between the two energy curves indicates good agreement.

Minimizations

For the validation of the phospho-amino-acid parameter set, MM minimizations of the model systems were performed in vacuo and explicit water. The resulting structures show good agreement with the ab initio optimized compounds in terms of bond lengths and angles (Table 3). Thus, the newly defined parameters perform well for minimizations in the gas phase as well as water.

Molecular dynamics

The main objective of this work was to develop parameters suitable for MD simulations of phosphorylated polypeptides in aqueous solution, which was verified by MD simulations of ten small model peptides, solvated in water. Energy values, temperature, and density were stable during the 1 ns MD runs. Molecular geometries showed no major distortions, and bond lengths and angles oscillated about their equilibrium values to an extent that is also expected for the unphosphorylated amino acids.

For the phosphate groups of phospho-amino-acid residues, free rotation around the *O*-phosphomonoester or phosphoramidate bond would be expected. MD simulation trajectories confirmed the occurrence of such a rotation during the MD runs. As shown in Fig. 3 for unprotonated and protonated phosphohistidine, dihedral angles of phosphate group oxygens interchanged in the course of the simulations. Values for the torsions O2-P-NA-CC and OH-P-NA-CC stayed close to the minimum values of the determined energy profiles (cf. Fig. 3).

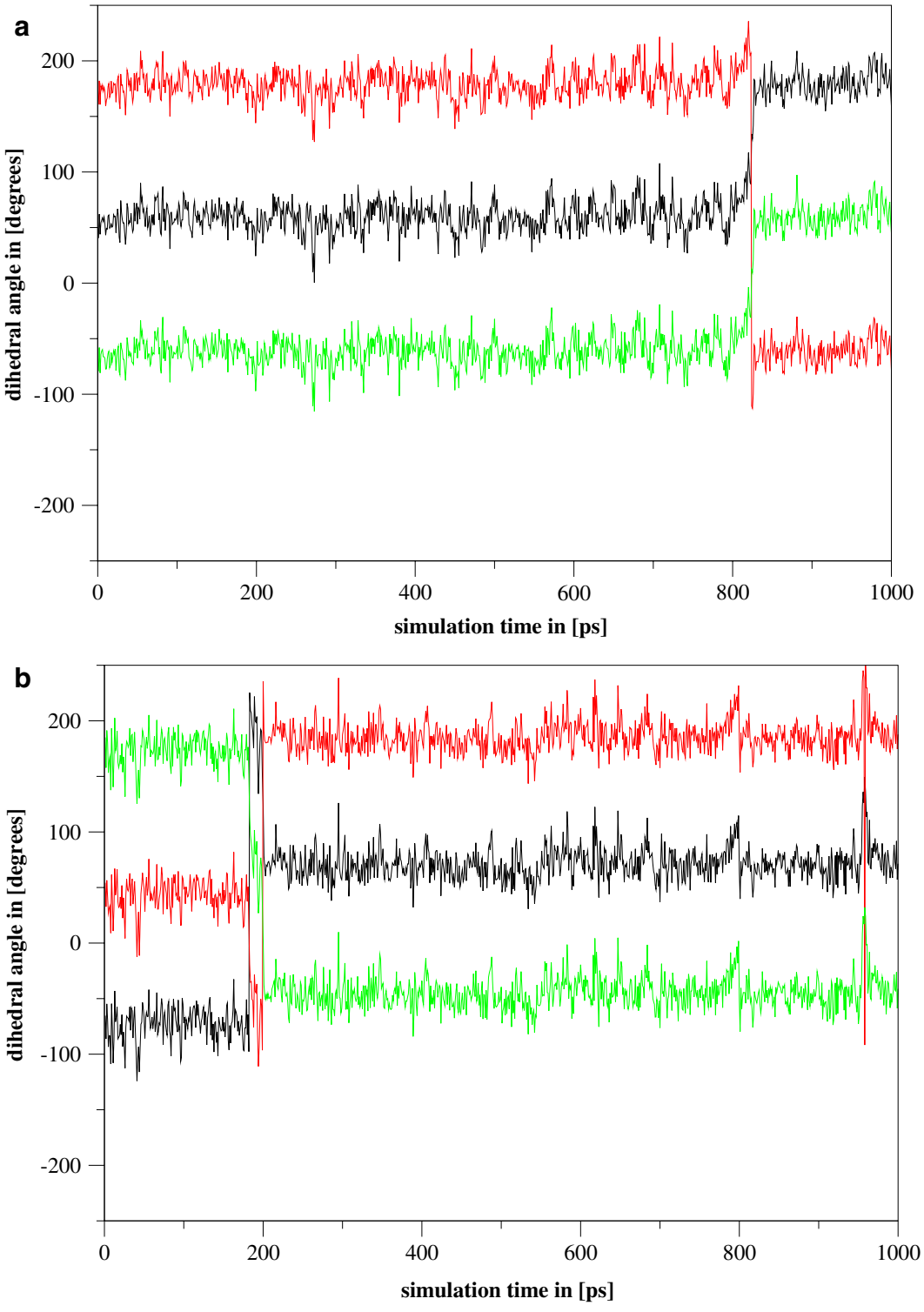

Fig. 3 Rotation of the phosphate group during MD simulation for ACE-HXD-NME model system. Shown are the three dihedral angles O2-P-NA-CC or OH-P-NA-CC, respectively, for (**a**) deprotonated and (**b**) protonated model system. Color-coding is according to the oxygen atoms of the phosphate group: O1P (*black*), O2P (*red*), O3P (*green*); cf. Fig. 1 for atom names

The results generally suggest good performance of our new parameters and an adequate consistency with the parm99 parameter set, thus providing a good basis for future investigations of phosphorylated proteins using AMBER. The new phospho-amino acid parameters are available through the internet [24].

Supplementary material available

RESP atomic charges for all residues are given in Tables S1a-e, and an overview of the parameter and library files available (for all ten phospho-amino acid residues for the use with the AMBER input preparation module LEAP) is shown in Table S2 of the Supplementary Material.

Acknowledgements The authors wish to thank Heike Meiselbach for helpful discussions, and the Leibnitz-Rechenzentrum in Munich and the Regionales Rechenzentrum Erlangen for computational resources. This work was supported by a grant from the Deutsche Forschungsgemeinschaft (SFB473, C10) to H. Sticht. N. Homeyer acknowledges a fellowship from the BioMedTec International Graduate School of Science (BIGSS), supported by the state of Bavaria.

References

1. Cohen P (2002) Nat Cell Biol 4:E127–E130
2. Tholey A, Lindemann A, Kinzel V, Reed J (1999) Biophys J 76:76–87
3. Titgemeyer F, Hillen W (2002) Antonie Van Leeuwenhoek 82:59–71
4. Klumpp S, Krieglstein J (2002) Eur J Biochem 269:1067–1071
5. Rajagopal P, Waygood EB, Klevit RE (1994) Biochemistry 33:15271–15282
6. Cheatham TE III, Cieplak P, Kollman PA (1999) J Biomol Struct Dyn 16:845–862
7. Cornell WD, Cieplak P, Bayly CI, Gould IR, Merz KM Jr, Ferguson DM, Spellmeyer DC, Fox T, Caldwell JW, Kollman PA (1995) J Am Chem Soc 117:5179–5197
8. Meagher KL, Redman LT, Carlson HA (2003) J Comput Chem 24:1016–1025
9. Young MA, Gonfloni S, Superti-Furga G, Roux B, Kuriyan J (2001) Cell 105:115–126
10. Wozniak E, Oldziej S, Ciarkowski J (2000) Comp Chem 24:381–390
11. Bienkiewicz EA, Lumb KJ (1999) J Biomol NMR 15:203–206
12. Cieplak P, Cornell WD, Bayly C, Kollman PA (1995) J Comput Chem 16:1357–1377
13. Easton RE, Giesen DJ, Welch A, Cramer CJ, Truhlar DG (1996) Theor Chim Acta 93:281–301
14. Ditchfield R, Hehre WJ, Pople JA (1971) J Chem Phys 54:724–728
15. Frisch MJ, Pople JA, Binkley JS (1984) J Chem Phys 80:3265–3269
16. Frisch MJ, Trucks GW, Schlegel HB, Scuseria GE, Robb MA, Cheeseman JR, Montgomery JA Jr, Vreven T, Kudin KN, Burant JC, Millam JM, Iyengar SS, Tomasi J, Barone V, Mennucci B, Cossi M, Scalmani G, Rega N, Petersson GA, Nakatsuji H, Hada M, Ehara M, Toyota K, Fukuda R, Hasegawa J, Ishida M, Nakajima T, Honda Y, Kitao O, Nakai H, Klene M, Li X, Knox JE, Hratchian HP, Cross JB, Bakken V, Adamo C, Jaramillo J, Gomperts R, Stratmann RE, Yazyev O, Austin AJ, Cammi R, Pomelli C, Ochterski JW, Ayala PY, Morokuma K, Voth GA, Salvador P, Dannenberg JJ, Zakrzewski VG, Dapprich S, Daniels AD, Strain MC, Farkas O, Malick DK, Rabuck AD, Raghavachari K, Foresman JB, Ortiz JV, Cui Q, Baboul AG, Clifford S, Cioslowski J, Stefanov BB, Liu G, Liashenko A, Piskorz P, Komaromi I, Martin RL, Fox DJ, Keith T, Al-Laham MA, Peng CY, Nanayakkara A, Challacombe M, Gill PMW, Johnson B, Chen W, Wong MW, Gonzalez C, Pople JA (2004) Gaussian 03. Gaussian Inc., Wallingford
17. Wang J, Cieplak P, Kollman PA (2000) J Comput Chem 21:1049–1074
18. Bayly CI, Cieplak P, Cornell WD, Kollman PA (1993) J Phys Chem 97:10269–10280
19. Case DA, Pearlman DA, Caldwell JW, Cheatham TE III, Wang J, Ross WS, Simmerling CL, Darden TA, Merz KM, Stanton RV, Cheng AL, Vincent JJ, Crowley M, Tsui V, Gohlke H, Radmer RJ, Duan Y, Pitera J, Massova I, Seibel GL, Singh UC, Weiner PK, Kollman PA (2002) Amber 7. University of California, San Francisco, CA
20. Wang J, Wolf RM, Caldwell JW, Kollman PA, Case DA (2004) J Comput Chem 25:1157–1174
21. Kosinsky YA, Volynsky PE, Lagant P, Vergoten G, Suzuki E, Arseniev AS, Efremov RG (2004) J Comput Chem 25:1313–1321
22. Hopfinger AJ, Pearlstein RA (1984) J Comput Chem 5:486–499
23. Jorgensen WL, Chandrasekhar J, Madura JD, Impey RW, Klein ML (1983) J Chem Phys 79:926–935
24. Bryce R, AMBER Parameter Database, http://pharmacy.man.ac.uk/amber/